Active stabilization for optically synchronized optical parametric chirped pulse amplification

Alexander Schwarz,[1,*] **Moritz Ueffing,**[1,3] **Yunpei Deng,**[1] **Xun Gu,**[1] **Hanieh Fattahi,**[1,2] **Thomas Metzger,**[1,2] **Marcus Ossiander,**[1,3] **Ferenc Krausz,**[1,2] **and Reinhard Kienberger**[1,3]

[1]*Max-Planck-Institute of Quantum Optics, Hans-Kopfermann-Straße 1, 85748 Garching, Germany*

[2]*Department of Physics, Ludwig-Maximilians-Universität München, Am Coulombwall 1, 85748 Garching, Germany*

[3]*Department of Physics, Technische Universität München, James Franck Straße, 85748 Garching, Germany*

[*]*alexander.schwarz@mpq.mpg.de*

Abstract: The development of new high power laser sources tends toward optical parametric chirped pulse amplification (OPCPA) in recent years. One of the difficulties in OPCPA is the the temporal overlap between pump and seed pulses. In this work we characterize our timing jitter on a single-shot basis using spectrally resolved cross-correlation in combination with a position sensitive detector. A commercial beam stabilization is adapted to actively enhance temporal overlap. This delay-stabilizer reduces the RMS jitter from $\sigma = 127\,\mathrm{fs}$ down to $\sigma = 24\,\mathrm{fs}$. The enhanced temporal overlap is demonstrated in our frontend and we propose the scheme to be applicable in many optically synchronized high-repetition-rate OPCPA systems.

OCIS codes: (140.3425) Laser stabilization; (140.7090) Ultrafast Lasers; (190.4970) Parametric oscillators and amplifiers.

References and links

1. I. N. Ross, P. Matousek, G. H. C. New, and K. Osvay, "Analysis and optimization of optical parametric chirped pulse amplification," J. Opt. Soc. Am. B **19**, 2945–2956 (2002).
2. B. C. Stuart, M. D. Feit, S. Herman, A. M. Rubenchik, B. W. Shore, and M. D. Perry, "Nanosecond-to-femtosecond laser-induced breakdown in dielectrics," Phys. Rev. B **53,** 1749–1761 (1996).
3. T. Metzger, A. Schwarz, C. Y. Teisset, D. Sutter, A. Killi, R. Kienberger, and F. Krausz,"High-repetition-rate picosecond pump laser based on a Yb:YAG disk amplifier for optical parametric amplification," Opt. Lett. **34,** 2123–2125 (2009).
4. S. Klingebiel, C. Wandt, C. Skrobol, I. Ahmad, S. A. Trushin, Z. Major, F. Krausz, and S. Karsch , "High energy picosecond Yb:YAG CPA system at 10 Hz repetition rate for pumping optical parametric amplifiers," Opt. Express **19,** 5357–5363 (2011).
5. M. Schulz, R. Riedel, A. Willner, T. Mans, C. Schnitzler, P. Russbueldt, J. Dolkemeyer, E. Seise, T. Gottschall, S. Hädrich, S. Duesterer, H. Schlarb, J. Feldhaus, J. Limpert, B. Faatz, A. Tünnermann, J. Rossbach, M. Drescher, and F. Tavella, "Yb:YAG Innoslab amplifier: efficient high repetition rate subpicosecond pumping system for optical parametric chirped pulse amplification," Opt. Lett. **36,** 2456–2458 (2011).
6. A. Pugzlys, G. Andriukaitis, A. Baltuska, L. Su, J. Xu, H. Li, R. Li, W. J. Lai, P. B. Phua, A. Marcinkevicius, M. E. Fermann, L. Giniunas, R. Danielius, and S. Alisauskas, "Multi-mJ, 200-fs, cw-pumped, cryogenically cooled,Yb,Na:CaF2 amplifier," Opt. Lett. **34,** 2075–2077 (2009).

#157288 - $15.00 USD Received 28 Oct 2011; revised 22 Dec 2011; accepted 10 Jan 2012; published 22 Feb 2012

7. K. Hong, A. Siddiqui, J. Moses, J. Gopinath, J. Hybl, F. Ilday, T. Fan, and F. Kärtner, "Generation of 287 W, 5.5 ps pulses at 78 MHz repetition rate from a cryogenically cooled Yb:YAG amplifier seeded by a fiber chirped-pulse amplification system," Opt. Lett. **33**, 2473–2475 (2008).
8. Zs. Major, S. Klingebiel, C. Skrobol, I. Ahmad, C. Wandt, S. A. Trushin, F. Krausz, and S. Karsch, "Status of the Petawatt Field Synthesizer pump-seed synchronization measurements," AIP Conference Proceedings **1228,** 117–122 (2010).
9. X. Gu, G. Marcus, Y. Deng, T. Metzger, C. Teisset, N. Ishii, T. Fuji, A. Baltuska, R. Butkus, V. Pervak, H. Ishizuki, T. Taira, T. Kobayashi, R. Kienberger, and F. Krausz, "Generation of carrier-envelope-phase-stable 2-cycle 740-μJ pulses at 2.1-μm carrier wavelength," Opt. Express **17,** 62–69 (2009).
10. D. Herrmann, L. Veisz, R. Tautz, F. Tavella, K. Schmid, V. Pervak, and F. Krausz, "Generation of sub-three-cycle, 16 TW light pulses by using noncollinear optical parametric chirped-pulse amplification," Opt. Lett. **34**, 2459–2461 (2009).
11. N. Ishii, C. Y. Teisset, T. Fuji, S. Köhler, K. Schmid, L. Veisz, A. Baltuska, and F. Krausz, "Seeding of an eleven femtosecond optical parametric chirped pulse amplifier and its Nd3+ picosecond pump laser from a single broadband Ti:sapphire oscillator, " IEEE J. Quantum Electron. **12,** 173–180 (2006).
12. T. R. Schibli, J. Kim, O. Kuzucu, J. T. Gopinath, S. N. Tandon, G. S. Petrich, L. A. Kolodziejski, J. G. Fujimoto, E. P. Ippen, and F. X. Kärtner, "Attosecond active synchronization of passively mode-locked lasers by balanced cross correlation," Opt. Lett. **28,** 947–949 (2003).
13. D. Yoshitomi, X. Zhou, Y. Kobayashi, H. Takada, and K. Torizuka, "Long-term stable passive synchronization of 50 μJ femtosecond Yb-doped fiber chirped-pulse amplifier with a mode-locked Ti:sapphire laser," Opt. Express **18,** 26027–26036 (2010).
14. T. Miura, K. Kobayashi and K. Takasago, Z. Zhang, K. Torizuka, and F. Kannari, "Timing jitter in a kilohertz regenerative amplifier of a femtosecond-pulse Ti:Al2O3 laser," Opt. Lett. **25,** 1795–1797 (2000).
15. J. Dörring, A. Killi, U. Morgner, A. Lang, M. Lederer, and D. Kopf, "Period doubling and deterministic chaos in continuously pumped regenerative amplifiers," Opt. Express **12**, 1759–1768 (2004).
16. Fastlite, "Dazzler references for insertion before or inside ultrafast amplifiers," www.fastlite.com/file/specs-before-amplis.pdf.
17. H. Fattahi, C. Skrobol, M. Ueffing, Y. Deng, A. Schwarz, Y. Kida, V. Pervak, T. Metzger, Z. Major, and Ferenc Krausz, "High efficiency, multi-mJ, sub 10 fs, optical parametric amplifier at 3 kHz," submitted for publication (2012).

1. Introduction

OPCPA is one path to push the boundaries in peak and average powers of current ultrashort lasers. As pointed out by Ross et. al [1], short pump pulses have advantages for OPCPA like short crystals and the associated broad bandwidths. Besides the process benefits from higher damage intensities [2]. But with the advent of new ultrashort high-energy pump-lasers for OPCPA [3–7], the synchronization between pump and seed pulses is getting more and more critical. Since rare-earth doped high-energy pump lasers usually exhibit a very narrow spectrum, they can not be used to seed broadband OPCPA. Therefore broadband Ti:Sapphire amplifier lasers are routinely used to achieve almost octave seed bandwidth [8–10]. These two laser amplifiers can be optically synchronized [11], meaning that both are seeded by the same broadband oscillator. Another approach is to electronically [12] or optically [13] synchronize two mode-locked oscillators, seeding their respective laser amplifiers.

With optical synchronization being a passive technique, slow temporal drifts as well as fast jitter in the laser amplifier systems are not compensated. In OPCPA, slow temporal drifts will cause the pump pulses to slip away from the optimum overlap with the seed. Fast jitter will not only decrease the pulse-to-pulse stability but also shift the amplified spectrum of the parametric amplification, leading to fluctuating pulse durations after the compression. This is why, on top of the passive optical synchronization, there is a need for actively enhanced synchronization performance.

2. Experimental realization

In this work we aim to improve the jitter performance of optical synchronization by an active feedback system, that has a potential bandwidth of many kHz. Also slow temporal drifts

#157288 - $15.00 USD Received 28 Oct 2011; revised 22 Dec 2011; accepted 10 Jan 2012; published 22 Feb 2012

in the laser setup will be compensated this way. To implement a spectrally resolved cross-correlation [14] in a spectrometer-like setup, we use position sensitive detectors (PSDs) to measure the delay between pump and seed for each shot. These PSDs are very sensitive to deviations of the center of mass and can be read out faster than a CCD array. Also sample&hold circuits are commercially available, making PSDs usable for kHz repetition rate systems. The commercial Aligna 4D (TEM Messtechnik, Hannover) is used to read out these PSDs and move a fast PID-regulated piezo stage. The device stays very versatile as it is based on commercial off-shelf products that are available for many different pulse energies, repetition rates or laser wavelengths.

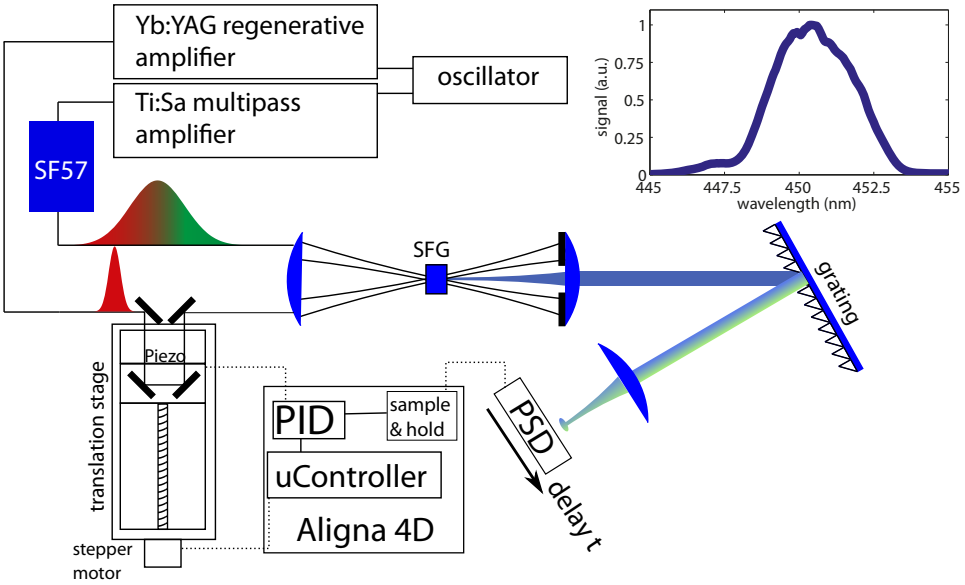

Fig. 1. Setup of the synchronization system. On the upper right, an averaged sum frequency spectrum is shown.

2.1. Optical setup

The setup is displayed in Fig. 1. We demonstrated the functionality by employing a broadband Ti:Sapphire multi-pass amplifier (Femtopower Compact Pro, Femtolasers) and a home-built picosecond Yb:YAG thin-disk regenerative amplifier (details see [3]). Both were optically synchronized as they derived their seed signal from an octave-spanning Ti:Sapphire oscillator (Rainbow, Femtolasers). Since the regenerative amplifier runs in an intermittent regime [15] where period doubling occurs, we have to switch its Pockels cells at twice the repetition rate of the Ti:Sapphire amplifier (3 kHz) and make sure that the amplified pulses of both lasers overlap (instead of occurring alternatively at twice the repetition rate). This is made sure when we increase the pump power of the regenerative amplifier by observing the two pulses on a standard oscilloscope. As soon as both pulses do overlap, the laser is able to run in this intermittent operation over the whole day.

For detecting the delay between pump and seed, a small portion of the broadband seed (about 2 mW) is stretched in bulk glass blocks (not shown in Fig. 1) of SF57 to a duration of about 5 ps. A mirror leakage of the compressed pump pulse (pulse duration 1.8 ps FWHM) with an energy of about 10 mW proves sufficient for the sum frequency generation (SFG) process. While the

#157288 - $15.00 USD Received 28 Oct 2011; revised 22 Dec 2011; accepted 10 Jan 2012; published 22 Feb 2012

original beams of pump and seed have a diameter of about 15 mm, for the limited apertures inside the SFG setup we are using telescopes which decrease the beam size to about 20 % and 40 % respectively. Using a plano-convex lens (focal length 100 mm), the seed ($\lambda \approx 800$ nm) and pump pulses ($\lambda = 1030$ nm) are overlapped in a quasi-collinear fashion inside a 1 mm thick BBO, cut at $\theta = 29^\circ$. Close matching of both foci (spot sizes both approximately 90 μm) ensures a strong sum frequency signal of about 0.2 mW at a wavelength of $\lambda \approx 450$ nm, which is recollimated and sent on a diffraction grating (1200 lines/mm, 45% diffraction efficiency). The residual seed and pump beams and their harmonics are blocked by an aperture. After focusing the beam from the grating onto the PSD with a 50 mm lens, the very elliptical focal spot translates temporal delay τ into spatial deviation in the direction of diffraction due to the temporal overlap of the pump pulse with different wavelength components of the stretched (chirped) seed pulse. This way imaging provides the frequency-space mapping, and the strong chirp of the pulse achieves the time-frequency mapping. Together, we have a time-space mapping. The spatial displacement on the PSD with respect to temporal delay is then given by

$$\frac{dx_{\mathrm{PSD}}}{d\tau} = \frac{\partial x_{\mathrm{PSD}}}{\partial \lambda_{\mathrm{SF}}} \frac{\partial \lambda_{\mathrm{SF}}}{\partial \omega_{\mathrm{seed}}} \frac{d\omega_{\mathrm{seed}}}{d\tau} \tag{1}$$

where on the right hand side the first term is given by the imaging system, the second by the seed and pump wavelengths in the SF process and the last by the stretching factor of the broadband seed. The parameters of the system are chosen such that the noise on x_{PSD} remains low. With small stretching factors $\frac{d\omega_{\mathrm{seed}}}{d\tau}$, the temporal resolution can be increased. However this sacrifices the range of the cross correlation and increases the spot-size on the PSD. Also the finite width of the pump pulse limits the achievable resolution. On the other hand, long stretching factors reduce the partial temporal overlap and therefore the signal on the PSD. The elevated electric noise then poses another limit to the temporal resolution. The perpendicular direction y_{PSD} shows a spatial jitter of below 0.7 μm in our system. Longer stretching of the seed or usage of a more dispersive grating could improve the signal-to-noise ratio, but here we are limited by the finite size of the PSD (4 mm). Since the spatial jitter equals a shift in delay of only 6 fs, these settings are regarded appropriate considering the resolution of the PSD (0.2 μm, Hamamatsu S599-01) and the noise in the connected signal processing electronics.

As the amplification cycle inside the regenerative amplifier takes 5 μs, temporal drifts are quite noticeable. They can not be attributed to either oscillator or regenerative amplifier, as we can only measure the relative delay between both. However, measuring the oscillator frequency with a RF frequency analyzer over several hours shows a significant contribution of the oscillator cavity length. These drifts are compensated by a translation stage (LIMES 84-120-HSM, OWIS) that centers the piezo voltage out of the PID regulator. The regulator reads out the displacement directly from the sample & hold electronics after the PSD and manipulates a fast piezo stage. With this hybrid solution, the limited range of the piezo stage (nanoX200, Piezosystems Jena, 240 μm range) only needs to compensate for fast jitter (> 10 Hz). Therefore we can keep the piezo resonance at a reasonable level (500 Hz with 40 g retroreflector weight) and the regulated bandwidth high as it is only limited by the piezo.

2.2. Long term drift

To demonstrate the amount of slow temporal drift experienced in our setup, Fig. 2 shows the movement of a delay stage that stabilized the SF spectral centroid by a (slow) software solution. The SF signal is kept over delays larger than the duration of the stretched seed by shifting the delay, which makes this measurement possible. On the left, one measurement per second is taken over 44 min while the lasers are warming up. Later the temporal drift then seems to oscillate, however the amplitude is still high compared to the pump pulse duration of 1.8 ps, as shown on the right of Fig. 2.

#157288 - $15.00 USD Received 28 Oct 2011; revised 22 Dec 2011; accepted 10 Jan 2012; published 22 Feb 2012

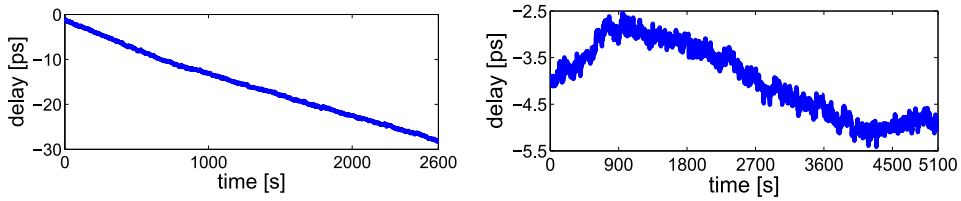

Fig. 2. Left: During the warm-up period a significant temporal drift can be observed. Right: After warming up, the delay starts oscillating.

As a useful by-product, the pulse duration of the pump laser can be calculated from the known dispersion factor D_λ (that needs to be reasonably large for this method). The measured FWHM of the pulse width (see inset in Fig. 1) is 3.3 ± 0.1 nm (averaged over 10000 samples), so a bulk dispersion of $D = 550 \frac{\text{fs}}{\text{nm}}$ gives us a pulse duration of 1.8 ps FWHM. Comparing to [3], the compressor setup for this work was rebuilt and not completely optimized, leading to a less perfect compression. The phase-matching bandwidth of our crystal is large enough not to affect the measurement considerably. This online characterization of the pump pulses proves useful in the day-to-day operation of the OPCPA setup.

2.3. Delay stabilization

We characterize the performance of our delay-stabilization using two approaches: Once we measure the error signal directly from the PSD, giving us noisier but single-shot signal for the temporal delay. The data is acquired using a digital storage oscilloscope that provides only 50 s of memory for the used sampling rate. For longer periods we have to rely on measurements of the SFG signal with a miniature spectrometer (HR 4000, Ocean Optics) using integration times of several milliseconds, therefore averaging dozens of laser pulses. This means for an integration time of 10 ms we are averaging out frequency components beyond 100 Hz and therefore measure a somewhat lower jitter. However the fast jitter components are characterized in the first shot-by-shot method already, here we mainly demonstrate long-term stability.

2.3.1. Performance of delay stabilization

Using the PSD error-signal, we can characterize our free-running jitter to be $\sigma = 127$ fs. This value was the average over several measurements as 50 s showed to be too short to characterize the fluctuating signal appropriately. To illustrate it in comparison with the stabilized results, a data set with $\sigma = 106$ fs is shown in Fig. 3a and Fig. 3b. Steep jumps are clearly visible (see Fig. 3a) and would lead to heavy fluctuations of the OPA center frequency and conversion efficiency. Furthermore the pulse-to-pulse jitter (taken from adjacent points) can be estimated to $\sigma = 15$ fs. This should be the lower achievable limit of the jitter between our lasers. For a lower repetition rate system our sampling would even be worse and accordingly the expected jitter should be higher in a comparable setup [8].

We use the implemented hardware delay stabilization to compensate jitter to a value of $\sigma =$ 24 fs (see Fig. 3), equivalent to 1.3 % of the pump pulse duration employing both piezo and stepper motor stages. Using the stepper motor alone, only $\sigma = 45$ fs can be achieved. The free running (blue) and the stabilized (green with piezo & stepper motor and red with stepper motor only) measurement are shown. An offset of ± 100 fs is used for better visibility.

Discrete Fourier transform of the measured data (see Fig. 3b) leads to a power spectral density P_f (not abbreviated as PSD in this manuscript) with equidistant and discrete frequencies

#157288 - $15.00 USD Received 28 Oct 2011; revised 22 Dec 2011; accepted 10 Jan 2012; published 22 Feb 2012

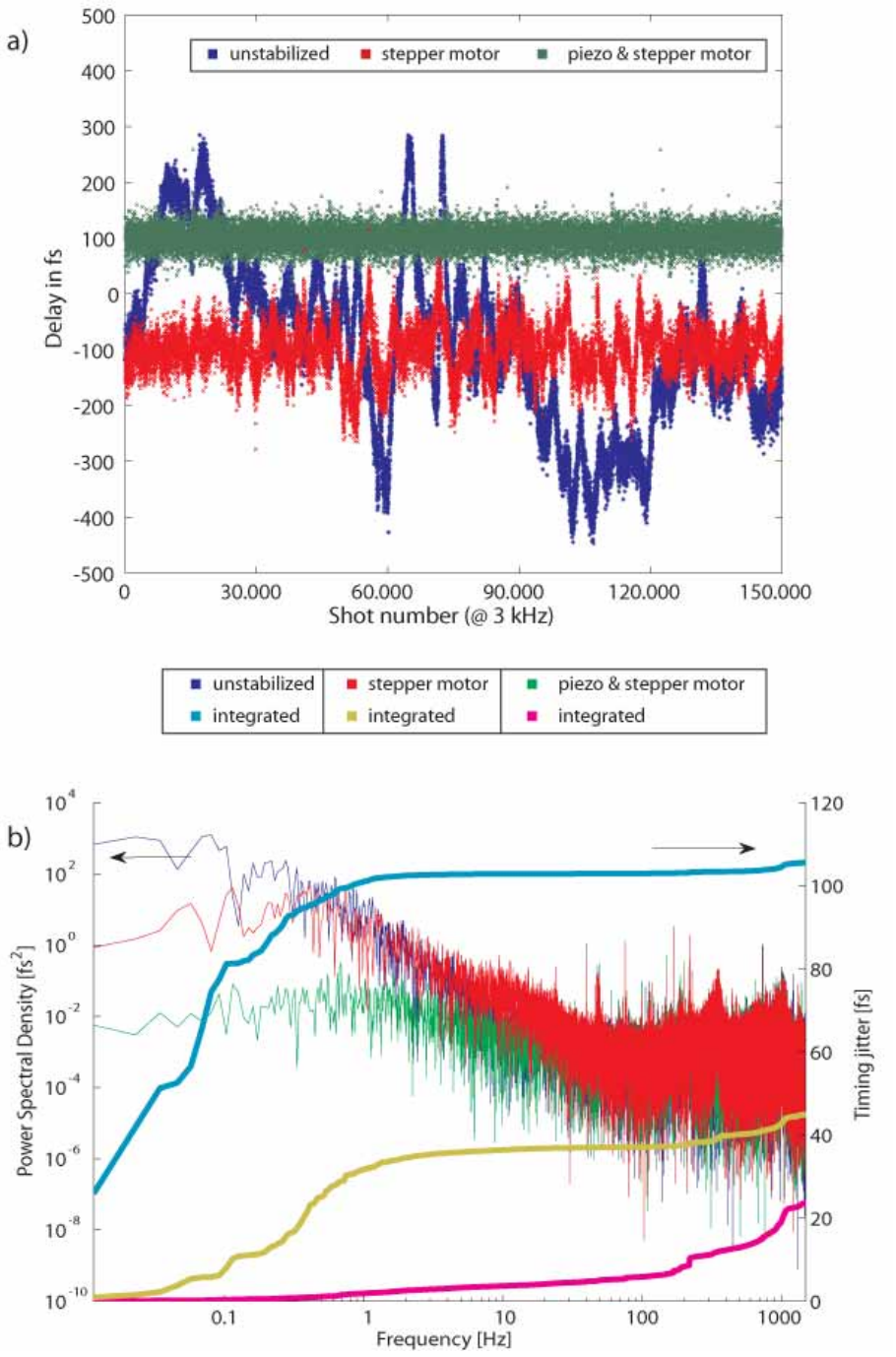

Fig. 3. (a) Measured delay based on frequency resolved SFG. The green and red curves are shifted by 100 fs for better visibility. (b) Fourier transform of the measured timing jitter. On the right scale the timing jitter is integrated.

#157288 - $15.00 USD Received 28 Oct 2011; revised 22 Dec 2011; accepted 10 Jan 2012; published 22 Feb 2012

$f = 0..1500\,\mathrm{Hz}$ (Nyquist frequency). The given jitter values are then calculated by $\sigma = \sqrt{\sum_f P_f}$.

The power spectral density shows a strong contribution around 220 Hz from the vibrations of beam stabilization piezos of another experiment. The fast piezo can remove higher frequency components, the slow stepper motor will only compensate temporal drifts. On the right ordinate, the integrated timing jitter is plotted. A steep increase at 220 Hz due to mechanical vibration on the optical table is clearly visible. As the main source of jitter for piezo-stabilization lies in the high frequencies beyond 220 Hz, the limit of performance accordingly seems to be influenced by fast mechanical vibrations and beam pointing. Also significant electronic noise from the lab is coupling into the readout electronic but could be reduced by a low pass filter with a cutoff around 10 kHz for this measurement. Note that the jitter values are still influenced by the pointing jitter observed on the PSD and should therefore contain a significant error (see discussion above). The signal-to-noise ratio, which is given from electronic noise in the electronics and beam-pointing on the PSD, comprises both the (PSD-based) measurement and the regulation. Also with higher PID values the high frequency jitter components increased. We explain this by insufficient mechanical fastening and sturdiness of the retroreflector on the piezo-driven stage.

Given the optical path length of $P_{OPL} \approx 1500\,\mathrm{m}$ inside the regenerative cavity, the resulting jitter may still be considered surprisingly low. A following multi-pass booster using identical thin-disk technology should not degrade this level significantly, as the path length would be increased only marginally.

2.3.2. Delay stabilization for OPCPA

To prove the improvement of timing jitter in an OPCPA stage, we measure the temporal jitter at a second independent setup. The schematic for stabilizing an OPCPA stage (or any kind of frequency conversion stage) is shown in Fig. 4. Different from the approach of [12], where two lasers are combined collinearly inside the control loop, the beams inside the OPCPA setup will only overlap at the crystals, meaning that fluctuations of both pump and seed arms will lead to induced temporal jitter. As with beam-pointing stabilizations, we can only stabilize to a virtual reference point. Everything beyond this point can not be compensated in the control loop (it is out-of-loop). Therefore, we see the need to measure the timing jitter out-of-loop in what could resemble a first OPCPA stage. For reasons of simplicity we copy the SFG setup rather than building an OPCPA stage that would require frequency doubling and a more complicated geometry. Furthermore we can compare in-loop and out-of-loop SFG signal simultaneously (as the phase-matching wavelength of both are offset) on the very same miniature spectrometer using a bifurcated delivery fiber. The center of mass for the spectra are plotted in Fig. 5 over a duration of 1228 s for the stabilized and unstabilized case. Note that both SFG (in-loop and out-of-loop) stages have temporal overlap and about the same path lengths overall, the path length out-of-loop is about 5 m. However telescopes in front of the in-loop SFG stage were employed to enhance the SFG efficiency. Therefore the beam pointing in both arms is different and we should expect a somewhat degraded temporal overlap in the external SFG stage. The same would hold for each OPA stage; the jitter is best compensated in the error signal but imperfect beam pointing leads to effective timing jitter at other points in the setup. Therefore we regard a jitter of $\sigma = 24\,\mathrm{fs}$ (as reported in 2.3.1) as the lower limit we can achieve with the current setup.

For the stabilized case the jitter in-loop can be reduced to a value of 15.6 fs (see Fig. 5, measured with the spectrometer), compared to the free-running (out-of-loop) jitter of 159.3 fs at this measurement. Of course the considerable jitter frequencies over 100 Hz (see Fig. 3b) are averaged out. The out-of-loop result of 21.9 fs shows however, that fluctuations outside the control loop are compensated to a high degree as well. As we do not expect our system to induce more shot-to-shot jitter, temporal overlap should therefore be very much improved out-of-loop.

The measured values are typical and depend on beam pointing and intensity fluctuations of

#157288 - $15.00 USD Received 28 Oct 2011; revised 22 Dec 2011; accepted 10 Jan 2012; published 22 Feb 2012

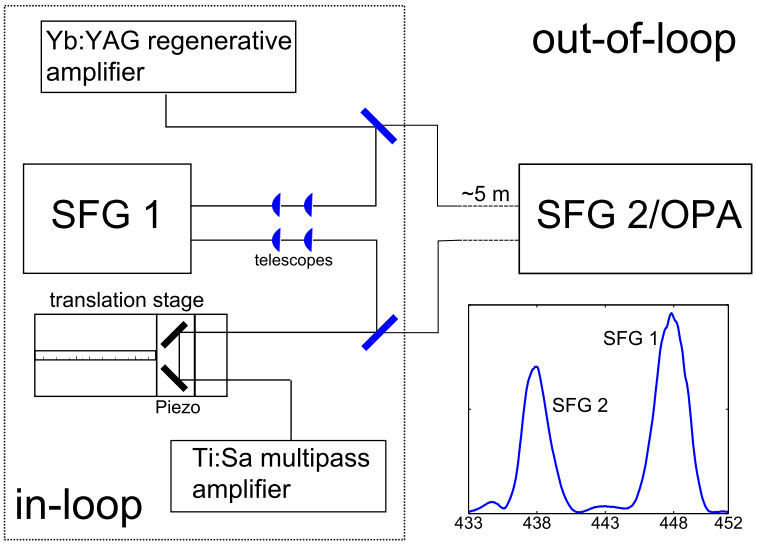

Fig. 4. Schematic for stabilizing an OPA stage. On the lower right inset, both SFG signals (averaged over 1000 shots) are shown on the same spectrometer.

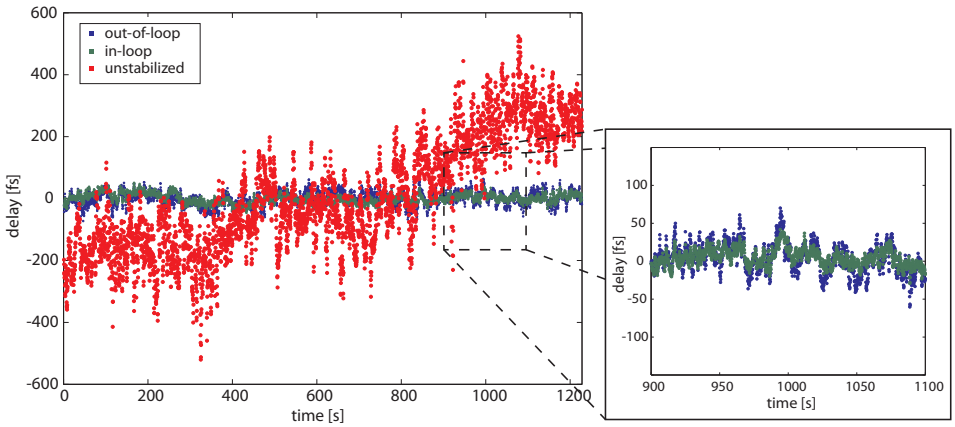

Fig. 5. Left: Jitter measured outside of the stabilization setup. Right: Detailed view, the delays in both SFG stages follow each other immediately.

both lasers, as well as on mechanical vibrations (in our case induced by vacuum pumps and piezo-driven actuators). Also we experience the regulators to work best with a very sharp SFG error signal, whereas double-spiked signals (as seen close to the edge of the SF phase-matching window) lead to worse performance. Both lasers warmed up for many hours before the measurement, but temporal drift is still significant over the measured period (see unstabilized plot in Fig. 5). From this measurement we conclude that over long periods, our temporal jitter can be held low as compared to the employed pump pulse duration and therefore temporal overlap in following OPA stages will be significantly improved. Further beam pointing stabilization of our pump laser should increase the performance even more in the near future and enable the use of sub-ps pump pulses in high energy amplifiers.

#157288 - $15.00 USD Received 28 Oct 2011; revised 22 Dec 2011; accepted 10 Jan 2012; published 22 Feb 2012

We can verify the observations of [13] that air turbulences did have a significant effect and could be reduced by covering beam paths. Temporal drifts as seen in Fig. 2 can also be clearly observed, however they are of no concern when employing the active delay stabilization. Vibrations as from vacuum pumps coupled to the optical table did show a very significant increase of timing jitter. In this case even the PSDs of our system vibrate, which makes it nearly impossible to measure or even stabilize correctly.

2.4. Versatility of the presented setup and outlook

Since our piezo stage is limited to a resonance frequency of 500 Hz, a short-stroke piezo element inside the regenerative amplifier could lead to improved feedback. Here we can take advantage of the many roundtrips inside the cavity, that otherwise would be expected to induce a significant amount of jitter. Higher repetition rate lasers could benefit even more from our approach, as they allow a higher sampling rate and could make the rather noisy sample&hold detection electronics obsolete. This would increase the resolution of the PSD even further. Using solid-state techniques, like an Acousto-Optic Programmable Dispersive Filter that comes in modern Ti:Sapphire amplifiers, jitter could be reduced at bandwidths in excess of 25 kHz [16] without any mechanical movement over a range of several picoseconds. At lower seed pulse energies, the cross-correlation by means of difference frequency generation can achieve higher gain as compared to SFG while being very moderate on the requirements of seed energy. Sidepulses in the SF spectrum would be suppressed even more rigorously this way, and the (possibly angularly dispersed) idler of a first (noncollinear) OPA stage would suffice.

3. Conclusion

In conclusion, active stabilization between pump and seed pulses of an optically synchronized OPCPA frontend was implemented. It could reduce the RMS timing jitter to $\sigma = 24$ fs and stabilizes external frequency conversion [17]. The device is inexpensive, reliable and should prove to be versatile in combination with ultrafast pump lasers at high repetition rates in the future.

Acknowledgments

We acknowledge technical support by T. Müller-Wirts and D. Chudjakov from TEM Messtechnik. R.K. acknowledges funding from an ERC Starting Grant. The work was supported by the cluster of excellence MAP.

#157288 - $15.00 USD Received 28 Oct 2011; revised 22 Dec 2011; accepted 10 Jan 2012; published 22 Feb 2012